Rapidity dependence of the average transverse momentum in hadronic collisions

F. O. Durães,[1] A. V. Giannini,[2] V. P. Gonçalves,[3,4] and F. S. Navarra[2]

[1]*Curso de Física, Escola de Engenharia, Universidade Presbiteriana Mackenzie CEP 01302-907 São Paulo, Brazil*

[2]*Instituto de Física, Universidade de São Paulo C.P. 66318, 05315-970 São Paulo, SP, Brazil*

[3]*Instituto de Física e Matemática, Universidade Federal de Pelotas Caixa Postal 354, CEP 96010-900 Pelotas, RS, Brazil*

[4]*Department of Astronomy and Theoretical Physics, Lund University, 223-62 Lund, Sweden*

(Received 16 May 2016; published 25 August 2016)

The energy and rapidity dependence of the average transverse momentum $\langle p_T \rangle$ in pp and pA collisions at energies currently available at the BNL Relativistic Heavy Ion Collider (RHIC) and CERN Large Hadron Collider (LHC) are estimated using the color glass condensate (CGC) formalism. We update previous predictions for the p_T spectra using the hybrid formalism of the CGC approach and two phenomenological models for the dipole-target scattering amplitude. We demonstrate that these models are able to describe the RHIC and LHC data for hadron production in pp, dAu, and pPb collisions at $p_T \leqslant 20$ GeV. Moreover, we present our predictions for $\langle p_T \rangle$ and demonstrate that the ratio $\langle p_T(y) \rangle / \langle p_T(y=0) \rangle$ decreases with the rapidity and has a behavior similar to that predicted by hydrodynamical calculations.

DOI: 10.1103/PhysRevC.94.024917

I. INTRODUCTION

The CERN Large Hadron Collider (LHC) has opened up a new frontier in high energy hadron-hadron collisions, allowing us to test the quantum chromodynamics in unexplored regimes of energy, density, and rapidities, considering different configurations of the colliding hadrons (protons and nuclei); for a recent review, see, e.g., Ref. [1]. In particular, the LHC experiments have unprecedented capacities to study several subjects associated with *forward physics* such as soft and hard diffraction, exclusive production of new mass states, low-x dynamics, and other important topics; for a review, see, Ref. [2]. Forward physics is characterized by the production of particles with relatively small transverse momentum, being traditionally associated with soft particle production, which is intrinsically nonperturbative and not amenable to first-principles analysis. However, in the particle production at large energies and forward rapidities, the wave function of one of the projectiles is probed at large Bjorken x and that of the other at very small x. The latter is characterized by a large number of gluons, which is expected to form a new state of matter—the color glass condensate (CGC)—where the gluon distribution saturates and nonlinear coherence phenomena dominate [1]. Such a system is endowed with a new dynamical momentum scale, the saturation scale Q_s, which controls the main features of particle production and whose evolution is described by an infinite hierarchy of coupled equations for the correlators of Wilson lines [3–5]. At large energies and rapidities, Q_s is expected to become much larger than the QCD confinement scale $\Lambda_{\rm QCD}$. Furthermore, the saturation scale is expected to determine the typical transverse momentum of the produced partons in the interaction. Consequently, the probe of the average transverse momentum $\langle p_T \rangle$ in hadronic collisions can provide important information about the QCD dynamics; for related studies, see Refs. [6–8].

Another motivation for a detailed analysis of $\langle p_T \rangle$ in pp and pA collisions is the recent suggestion made in Ref. [9] that this quantity can be used to disentangle the hydrodynamic and the CGC descriptions of the "ridge" effect (the appearance of long-range correlations in the relative pseudorapidity $\Delta\eta$ and the relative azimuthal angle $\Delta\phi$ plane) observed in high-multiplicity events in small colliding systems such as pp and $p(d)A$ [10–17]. While the previously ridge-type structure observed in heavy-ion collisions at the BNL Relativistic Heavy Ion Collider (RHIC) and the LHC was considered as evidence of the hydrodynamical nature of the quark-gluon plasma (see Refs. [18,19]) there is no compelling reason why small systems should also exhibit a hydrodynamical behavior even though a hydrodynamic approach is able to describe the experimental data [20,21]. On the other hand, the CGC approach also provides a qualitatively good description of the same data [22–32]. Therefore, the origin of the ridge in pp and pA collisions is still an open question. As the ridge effect, the azimuthal asymmetries observed in pPb collisions at the LHC energies by the ALICE [12], ATLAS [13,33], and CMS [11,17] collaborations are also open to different theoretical explanations. While in the hydrodynamic approaches those anisotropies emerge as a final-state feature due to the hydrodynamic flow [20,21,34], in the CGC approach they are described as initial state anisotropies which are present at the earliest stages of the collision [35]. In Ref. [9], the authors have studied the rapidity (y) dependence of the average transverse momentum of charged particles using very general arguments that lead to simple analytical expressions. In particular, the Golec-Biernat-Wusthoff (GBW) model [36] was used to describe the unintegrated gluon distribution, and the fragmentation of the partons into final-state particles was neglected. The authors of [9] have found that the average transverse momentum $\langle p_T \rangle$ in the CGC approach grows with rapidity, in contrast to what is expected from a collective expansion. Indeed, the hydrodynamical model predicts a decrease of the average transverse momentum when going from midrapidity, $y = 0$, to the proton side, owing to a decreasing number of produced particles. The prediction of these distinct behaviors is one the main motivations for the detailed analysis of the energy and rapidity dependencies

of $\langle p_T \rangle$ and thus needed to verify the robustness of this conclusion. Because the GBW model does not describe the p_T spectra measured in pp and pA collisions, in our study we will consider two more realistic phenomenological saturation models that are able to reproduce the experimental data in the region of small transverse momenta. This is the region that determines the behavior of the average transverse momentum. Moreover, we will analyze the impact of the inclusion of parton fragmentation in the rapidity dependence of $\langle p_T \rangle$. With these improvements, we are able to present realistic predictions for $\langle p_T \rangle$ based on the CGC results that are able to describe the current experimental data on hadron production in hadronic collisions.

This paper is organized as follows. In the next section we present a brief review of the hybrid formalism and discuss the phenomenological models of the dipole scattering amplitudes used in our analysis. In Sec. III we update the main parameters of these phenomenological models by the comparison with RHIC and LHC data on hadron production in pp, dAu, and pPb collisions. Using the new version of these models, which are able to describe the experimental data for $p_T \leqslant 20$ GeV, we present our predictions for the rapidity and energy dependencies of the average transverse momentum in pp and pPb collisions. Finally, in Sec. IV we summarize our main conclusions.

II. PARTICLE PRODUCTION IN THE CGC: HYBRID FORMALISM

To estimate the energy and rapidity dependencies of the average transverse momentum $\langle p_T \rangle$ we will need to describe particle production at forward rapidities and large energies. The description of hadron production at large transverse momentum p_T is one the main examples of a hard process in perturbative QCD (pQCD). It can be accurately described within collinear factorization, by combining partonic cross sections computed to some fixed order in perturbation theory with parton distribution and fragmentation functions whose evolution is computed by solving the Dokshitzer-Gribov-Lipatov-Altarelli-Parisi (DGLAP) equations [37] to the corresponding accuracy in pQCD. The high transverse momentum p_T of the produced hadron ensures the applicability of pQCD, which is expected to fail to low p_T^2. Furthermore, at forward rapidities the small-x evolution becomes important, leading to a growth of the gluon density and of the gluon transverse momentum. Because of that, in this kinematical range their evolution in transverse momentum cannot be disregarded, which implies that at very forward rapidities the collinear factorization is expected to break down. An alternative is the description of hadron production using the k_T factorization scheme, which is based on unintegrated gluon distributions whose evolution is described by the Balitsky-Fadin-Kuraev-Lipatov (BFKL) equation [38]. However, if the transverse momentum of some of the produced particles is comparable with the saturation momentum scale, the partons from one projectile scatter off a dense gluonic system in the other projectile. In this case the parton undergoes multiple scatterings, which cannot be encoded in the traditional (collinear and k_T) factorization schemes. As pointed in Ref. [39], the forward hadron production in hadron-hadron collisions is a typical example of a dilute-dense process, which is an ideal system for studying the small-x components of the target wave function. In this case the cross section is expressed as a convolution of the standard parton distributions for the dilute projectile, the dipole-hadron scattering amplitude (which includes the high-density effects), and the parton fragmentation functions. Basically, assuming this generalized dense-dilute factorization, the minimum bias invariant yield for single-inclusive hadron production in hadron-hadron processes is described in the CGC formalism by [40]

$$\frac{dN_h}{dyd^2p_T} = \frac{K(y)}{(2\pi)^2}\int_{x_F}^1 dx_1\,\frac{x_1}{x_F} \times\left[f_{q/p}(x_1,\mu^2)\widetilde{\mathcal{N}}_F\left(\frac{x_1}{x_F}p_T,x_2\right)D_{h/q}\left(\frac{x_F}{x_1},\mu^2\right) + f_{g/p}(x_1,\mu^2)\widetilde{\mathcal{N}}_A\left(\frac{x_1}{x_F}p_T,x_2\right)D_{h/g}\left(\frac{x_F}{x_1},\mu^2\right)\right], \tag{1}$$

where p_T, y, and x_F are the transverse momentum, rapidity, and Feynman x of the produced hadron, respectively. The $K(y)$ factor mimics the effect of higher order corrections and, effectively, of other dynamical effects not included in the CGC formulation. The variable x_1 denotes the momentum fraction of a projectile parton, $f(x_1,\mu^2)$ the projectile parton distribution functions, and $D(z,\mu^2)$ the parton fragmentation functions into hadrons. These quantities evolve according to the DGLAP evolution equations [37] and obey the momentum sum rule. It is useful to assume $\mu^2 = p_T^2$. Moreover, $x_F = \frac{p_T}{\sqrt{s}}e^y$ and the momentum fraction of the target partons is given by $x_2 = x_1 e^{-2y}$ (for details, see [40]). In Eq. (1), $\widetilde{\mathcal{N}}_F(x,k)$ and $\widetilde{\mathcal{N}}_A(x,k)$ are the fundamental and adjoint representations of the forward dipole amplitude in momentum space and are given by

$$\widetilde{\mathcal{N}}_{A,F}(x,p_T) = \int d^2r\, e^{i\vec{p}_T\cdot\vec{r}}[1-\mathcal{N}_{\mathcal{A},\mathcal{F}}(x,r)]\,, \tag{2}$$

where $\mathcal{N}_{\mathcal{A},\mathcal{F}}(x,r)$ encodes all the information about the hadronic scattering, and thus about the nonlinear and quantum effects in the hadron wave function. Following [41], we will assume in what follows that $\mathcal{N}_F(x,r)$ can be obtained from $\mathcal{N}_A(x,r)$ after rescaling the saturation scale by $Q_{s,F}^2 = (C_F/C_A)Q_{s,A}^2$ where $C_F/C_A = 4/9$. In principle, we should also include in Eq. (1) the inelastic term that has been calculated in [42]. This term accounts for part of the full next-to-leading-order correction to the hybrid formalism which was recently presented in [43,44]. It has also been shown recently [45] that the inclusion of this term modifies the shape of the p_T spectra. However, we are concerned only with the average transverse momentum $\langle p_T \rangle$ (and its rapidity dependence) and this term plays a negligible role in this observable, which is dominated by the low-p_T part of the spectra. Because of this reason we will omit this term in our analysis.

In general the scattering amplitude $\mathcal{N}_A(x,r)$ can be obtained by solving the Balitsky-Kovchegov (BK) evolution equation [3,4]. The BK equation is the simplest nonlinear evolution equation for the dipole-hadron scattering amplitude,

being actually a mean-field version of the first equation of the Jalilian-Marian–Iancu–McLerran–Weigert–Leonidov–Kovner (JIMWLK) hierarchy [3,5]. Over the last few years, several authors have studied the solution of the BK equation including higher order corrections [46–48] and used it as input in the analysis of leading hadron production in pp and pA collisions, obtaining a very good description of the experimental data [45,50,51]. In what follows, instead of the solution of the BK equation, we will consider two different phenomenological models based on the analytical solutions of this equation. This allows us to investigate the possibility of getting insight into whether the LHC data are sensitive to geometric scaling violations at high values of p_T.

Moreover, as these phenomenological models differ from the GBW model in the dependence of the anomalous dimension with the momentum scale (see below), it becomes possible to clarify the origin of the differences between the predictions. Such analysis is a hard task when the numerical solution of the BK equation is considered as input to the calculations. Our phenomenological approach has limitations, being valid only in a limited region of transverse momenta and not being competitive with recent parametrizations that are being used to describe the nuclear modification ratio R_{pA} [45,49–52]. As demonstrated in those references, a precise treatment of the nuclear geometry and/or the initial conditions is necessary to describe the ratio R_{pA}. Such aspects are beyond the scope of this paper.

On the other hand, since $\langle p_T \rangle$ is determined by the region of small p_T, the use of phenomenological models that describe the experimental data in this kinematical range allows us to obtain realistic predictions for this quantity. It is well known that several groups have constructed phenomenological models for the dipole scattering amplitude using the RHIC data and/or data from the Hadron-Electron Ring Accelerator (HERA) at DESY to fix the free parameters [40,41,53,54]. In general, it is assumed that $\mathcal{N}$ can be modeled through a simple Glauber-like formula,

$$\mathcal{N}(x,r_T) = 1 - \exp\left[-\tfrac{1}{4}\left(r_T^2 Q_s^2\right)^{\gamma}\right], \tag{3}$$

where γ is the anomalous dimension of the target gluon distribution. The speed with which we move from the nonlinear regime to the extended geometric scaling regime and then from the latter to the linear regime is what differs one phenomenological model from another. This transition speed is dictated by the behavior of the anomalous dimension $\gamma(x,r_T^2)$. In the GBW model, γ is assumed to be constant and equal to unity. In this paper we will consider the dipole models proposed in Refs. [40,41] to describe the p_T spectra of particle production at RHIC. In the DHJ model [40], the anomalous dimension was proposed to be given by

$$\gamma(x,r_T)_{\rm DHJ} = \gamma_s + (1-\gamma_s)\frac{\left|\ln\left(1/r_T^2 Q_s^2\right)\right|}{\lambda y + d\sqrt{y} + \left|\ln\left(1/r_T^2 Q_s^2\right)\right|}, \tag{4}$$

with $Q_s^2 = A^{1/3} Q_0^2 (x_0/x_2)^{\lambda}$, $\gamma_s = 0.628$, $Q_0^2 = 1.0$ GeV^2, $x_0 = 3.0 \times 10^{-4}$, $\lambda = 0.288$, and $d = 1.2$. This model was designed to describe the forward dAu data at the RHIC highest energy taking into account geometric scaling violations characterized by terms depending on the target rapidity, $y = \ln(1/x_2)$, in its parametrization of the anomalous dimension, with the parameter d controlling the strength of the subleading term in y. In contrast, in the BUW model [41] the anomalous dimension is given by

$$\gamma(\omega = q_T/Q_s)_{\rm BUW} = \gamma_s + (1-\gamma_s)\frac{(\omega^a - 1)}{(\omega^a - 1) + b}, \tag{5}$$

where $q_T = p_T/z$ is the parton momentum. The parameters of the model ($\gamma_s = 0.628$, $a = 2.82$, and $b = 168$) have been fixed by fitting the p_T spectra of the produced hadrons measured in pp and dAu collisions at the RHIC energies [41,55]. With these parameters the model was also able to describe the ep HERA data for the proton structure function if the light quark masses are neglected. An important feature of this model is the fact that it explicitly satisfies the property of geometric scaling [56–58] which is predicted by the solutions of the BK equation in the asymptotic regime of large energies. Since the forward RHIC data for the p_T spectra are reproduced by both models [40,41], it was not possible to say whether experimental data show violations of the geometric scaling or not. In principle, it is expected that by considering the transverse momentum distribution of produced hadrons measured at the LHC energies it should be possible to address this question since the new data are taken at a wider range of p_T when compared to the RHIC data.

Finally, it is important to emphasize that the different behavior of the anomalous dimension, present in the GBW, DHJ, and BUW models, also implies a distinct x dependence of the scattering amplitude. In particular, the onset of saturation is different in these models, with the GBW one predicting a faster onset (in comparison to the other models) which is disfavored by recent analysis of the HERA data (see, e.g., Ref. [60]). These different behaviors have a direct impact on the rapidity dependence of the particle production cross section in hadronic collisions. Moreover, the GBW model implies an exponential behavior for $\widetilde{\mathcal{N}}_{A,F}(x,p_T)$ and, as a consequence, for the p_T dependence of the cross sections, which disagrees with the power-law behavior observed in the experimental data. An illustration of this disagreement can be found in Ref. [61]. Such unrealistic behavior is cured in the BUW and DHJ by modeling the anomalous dimension, taking into account the dependence on the energy and on the dipole pair size. Such dependencies agree with the results obtained by the solution of the rcBK equation [46].

III. RESULTS AND DISCUSSION

In what follows we will present our results for the average transverse momentum $\langle p_T \rangle$ defined by

$$\langle p_T \rangle = \frac{\int d^2p_T\, p_T \frac{dN_h}{dyd^2p_T}}{\int d^2p_T \frac{dN_h}{dyd^2p_T}}, \tag{6}$$

which is rapidity and energy dependent, i.e., $\langle p_T \rangle = \langle p_T(y,\sqrt{s}) \rangle$. Moreover, it depends of the lower limit of the integrations over the transverse momentum ($p_{T,\rm min}$). To obtain realistic predictions for LHC energies it is fundamental to use as input in the calculations a model which describes the

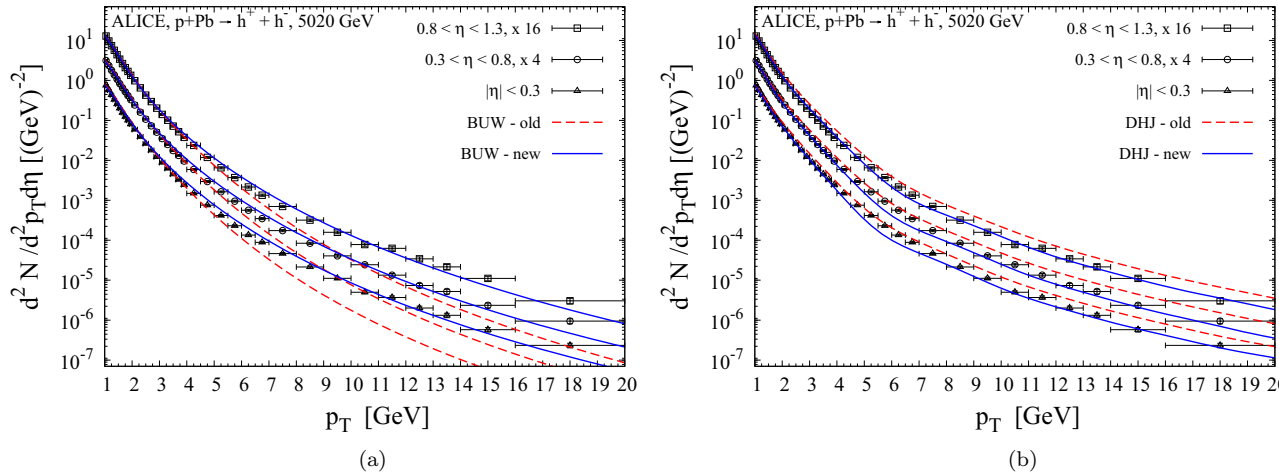

FIG. 1. Comparison between the (a) BUW and (b) DHJ predictions for the transverse momentum p_T spectra of charged particles produced in pPb collisions and the ALICE data [59]. For the new version of the BUW model we assume $K = 3.7$ for all pseudorapidity bins and for the new DHJ model $K = 3.0$, 3.0, and 3.7 for $\langle\eta\rangle = 0$, 0.55, and 1.05, respectively.

experimental data on the p_T spectra of produced particles at different rapidities. Consequently, as a first step we will initially compare the DHJ and BUW predictions with the recent LHC data. In Fig. 1 we present a comparison of these predictions using the original parameters, denoted "DHJ old" and "BUW old" in the figures, with the LHC data on the p_T spectra of charged particles in pPb collisions at $\sqrt{s} = 5.02$ TeV and different rapidities [59]. We use in what follows the CTEQ5L parton distribution functions [62] and the KKP fragmentation functions [63], with the hadron mass being chosen to be the mean value of the pion, kaon, and proton masses. Moreover, we compute Eq. (1) using the central values of η in the pseudorapidity ranges used in the experiment and choose $A \equiv A_{\text{min. bias}} = 20$ (18.5) for pPb (dAu) collisions. We find that these models are not able to describe the ALICE data [59] at large transverse momentum with their original parameters. The natural next step is to check if a new fit of the free parameters of these models can improve the description of the experimental data. Because one of the goals of our paper is to check if the average transverse momentum can be used to discriminate between the CGC and hydrodynamic descriptions of high-multiplicity events observed in pPb collisions at LHC, our strategy will be the following: to determine the free parameters of the BUW and the DHJ dipole scattering amplitudes by fitting the p_T spectra of charged particles measured in pPb collisions at $\sqrt{s} = 5020$ GeV and then compare the new models with the experimental data on pp and dAu collisions at other energies and rapidities. Moreover, differently from the authors of Refs. [40,41], who have assumed that $\gamma_s \approx 0.63$, which is the value obtained from the leading-order BFKL kernel, we will consider γ_s as a free parameter. We will consider the experimental data in the rapidity ranges: $|\eta| < 0.3$,$0.3 < \eta < 0.8$ and $0.8 < \eta < 1.3$. Consequently, the results from these models at larger rapidities should be considered as predictions. It is important to emphasize that the fit of the p_T spectra at a given rapidity constrains the parameters that determine the anomalous dimension of the model. Therefore, they determine the rapidity dependence of the scattering amplitude, as can be observed in Eq. (3), and as a consequence, the η dependence of the production cross sections. The resulting fits are shown in Figs. 1(a) and 1(b) for the following parameters: $a = 2.0$, $b = 125$, and $\gamma_s = 0.74$ for the BUW model and $d = 1.0$ and $\gamma_s = 0.7$ for the DHJ model. The data are better described if we assume larger values of $\gamma_s \geqslant 0.7$, which is consistent with the results obtained using the renormalization group improved BFKL kernels at next-to-leading order and fixed running coupling [64]. As it can be seen, with these parameter sets our curves agree well with the experimental data. In the range $4 < p_T < 7$ GeV the DHJ curves show an "edgy" behavior which is reminiscent of the numerical Fourier transform. This is not a big effect and can be considered as part of the theoretical error in our calculations. It is important to emphasize that $\langle p_T\rangle$ is only marginally affected by these small oscillations (see below) and the qualitative fits presented here for both models considered are sufficient to get a realistic prediction for this observable since it is dominated by the low-p_T region.

Having fixed the new parameters of the BUW and DHJ models using the experimental data on hadron production in pPb collisions, we now compare their predictions with the recent LHC data on p_T spectra of charged particles and neutral pions measured in pp collisions at different energies and distinct rapidity ranges. The only free parameter in our predictions is the K factor, which can be energy and rapidity dependent. In what follows we will fix this parameter in order to describe the experimental data at lower p_T. In Fig. 2 we present our results. We observe that both models describe quite well the experimental data for small p_T, with the BUW predictions becoming worse at higher p_T with increasing center-of-mass energy. In contrast, the DHJ model also describes quite well data of larger p_T, which can be associated with the contribution of the geometric scaling violations taken into account in this model.

As a final check, let us compare the predictions of these new versions of the phenomenological models with the RHIC data on hadron production in pp and dAu collisions in the central and forward rapidity regions. This comparison allows us to

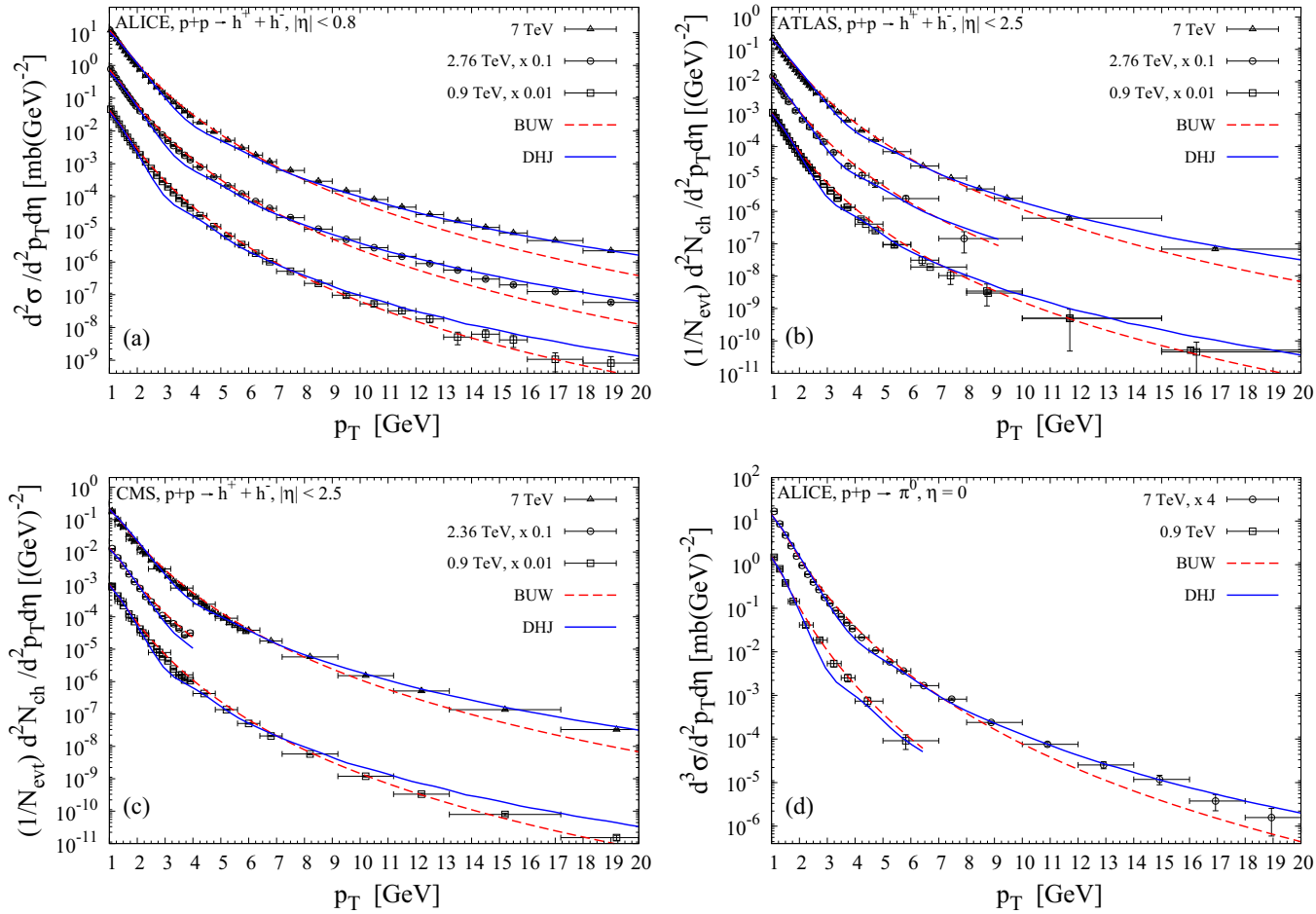

FIG. 2. Predictions of the DHJ and BUW models for the p_T spectra of charged particles in pp collisions. (a) Comparison with the ALICE data [65]. The corresponding K factors are the following: $K = 2.47$ ($K = 2.3$), 2.07 (1.85), and 1.77 (1.6) for the BUW (DHJ) model for $\sqrt{s} = 0.9$, 2.76, and 7 TeV. (b) Comparison with the ATLAS data [66]. In this case we have assumed $K = 3.3$, 2.5, and 2.3, respectively, for both models. (c) Comparison with the CMS data [67]. In this case we assume for both models $K = 3.0$, 2.5, and 2.3 for $\sqrt{s} = 0.9$, 2.36, and 7 TeV. (d) Predictions of the DHJ and BUW models for the p_T spectra of neutral pions. Comparison with the ALICE data [68] for $\sqrt{s} = 0.9$ and 7 TeV. For both models we have $K = 1.2$ and 2.0.

check if these models predict the correct η dependence of the production cross sections. In Figs. 3(a) and 3(b) we present our predictions. We find that both models describe well the experimental data at forward rapidities. On the other hand, at central rapidities, the BUW describes well the pp data for $p_T \leqslant 10$ GeV, but fails for $p_T \geqslant 3$ GeV in the case of dAu collisions. In contrast, the results of the DHJ model are not shown for these rapidities since they are highly affected by oscillations for $p_T \gtrsim 5$ GeV. The failure of the description at central rapidities at RHIC is not surprising since the energy is not very large and the formalism used here is suited to the study of the forward region where the small-x component of the target wave function is accessed. Finally, in Fig. 3(c) we demonstrate that the new version of the BUW model satisfies the property of the geometric scaling and also is able to describe the ep HERA data for the total $\gamma^* p$ cross section in a large range of photon virtualities.

The results presented in Figs. 1–3 make us confident in obtaining realistic predictions for the average transverse momentum. In what follows we will study the energy and rapidity dependencies of the ratio

$$R = \frac{\langle p_T(y,\sqrt{s})\rangle}{\langle p_T(0,\sqrt{s})\rangle}, \tag{7}$$

where the denominator represents the average transverse momentum at zero rapidity. The motivation to estimate this ratio is the reduction of the uncertainties related to the fragmentation functions as well as in the choice of the minimum transverse momentum present in the calculation of $\langle p_T\rangle$. Initially, let us analyze the dependence of our predictions on the model used to describe the forward scattering amplitudes $\mathcal{N}_{\mathcal{A},\mathcal{F}}(x,r)$ and the impact of the inclusion of parton fragmentation. In Fig. 4 we compare the predictions of the BUW and DHJ models with those from the GBW model [36], obtained assuming $p_{T,\min} = 1$ GeV. It is important to emphasize that the GBW model is not able to describe the experimental data on hadron production in hadronic collisions, since it predicts that $\mathcal{N}_{\mathcal{A},\mathcal{F}}(x,r)$ decreases exponentially at large transverse momentum. However, as this model is usually considered to obtain analytical results for several observables, we would like

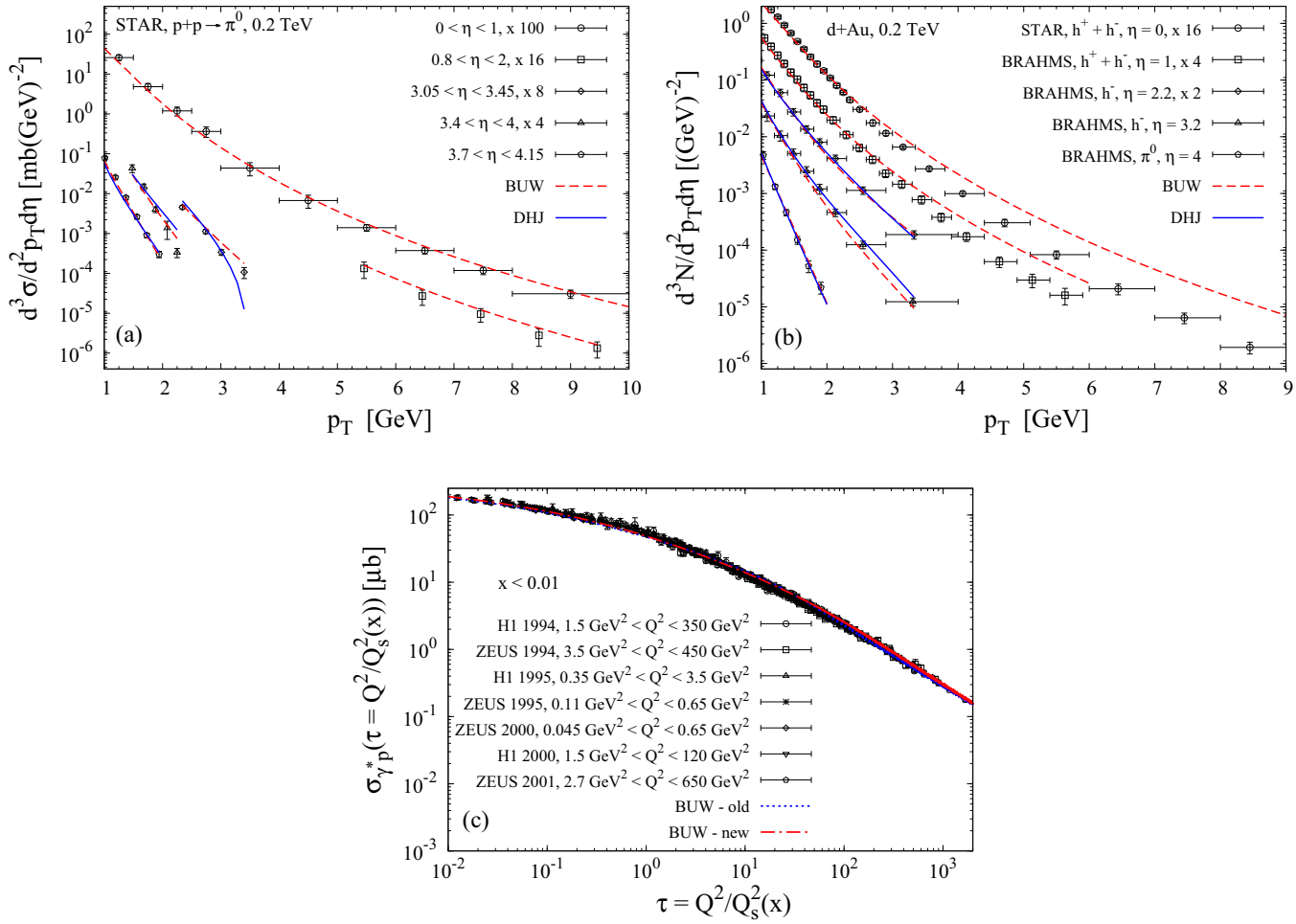

FIG. 3. (a) Predictions of the DHJ and BUW models for the p_T spectra of neutral pions in pp collisions. For the BUW model $K = 1.5$ for $\langle\eta\rangle = 0.5$ and $K = 1.2$ for $\langle\eta\rangle = 1.4$, 3.25, 3.7, and 3.925. For the DHJ model $K = 1.2$ for $\langle\eta\rangle = 3.25$,3.7,3.925. The experimental data are from [69]. (b) Predictions of the DHJ and BUW models for the p_T spectra of hadron production in dAu collisions. For the BUW model we have $K = 2.9$, 2.5, 2.0, 1.0, and 1.0 for $\eta = 0$, 1, 2.2, 3.2, and 4, respectively. For the DHJ model we have $K = 2.5$, 2.4, and 1.5 for $\eta = 2.2$, 3.2, and 4, respectively. The experimental data are from [70]. (c) Comparison between the BUW predictions and the ep HERA data for the total $\gamma^* p$ cross section [71].

to verify if its predictions for $\langle p_T\rangle$ are realistic. In Figs. 4(a) and 4(c) we present our predictions disregarding parton fragmentation, while in Figs. 4(b) and 4(d) fragmentation is included. It is important to emphasize that our results for the GBW model without fragmentation, obtained using the hybrid formalism, are similar to those obtained in Ref. [9] with the k_T-factorization approach. We can see that the DHJ and BUW predictions are similar (to each other) and differ significantly from the GBW one. While the GBW model predicts a growth of the ratio for $y \leqslant 6$, the BUW and DHJ models predict that this ratio is almost constant or decreases with rapidity. This distinct behavior is due to the fact that the anomalous dimension of the GBW model is equal to unity. This implies an energy dependence of the scattering amplitude which is stronger in the GBW than in the other models, where $\gamma < 1$. The energy dependence of $\widetilde{\mathcal{N}}_{A,F}(x, p_T)$ determines the behavior with rapidity of the production cross sections and, consequently, of the average transverse momentum. The predictions of the GBW model have a stronger rapidity dependence. In this model there is a faster onset of saturation which is not supported by the experimental data. The inclusion of parton fragmentation is presented in Figs. 4(b) and 4(d). As can be seen, fragmentation modifies the rapidity dependence of the average transverse momentum, implying a smaller growth of the GBW prediction. In the case of the DHJ and BUW predictions, the inclusion of fragmentation implies that the fall of the ratio begins at smaller rapidities.

Our results demonstrate that the inclusion of fragmentation has an important impact on the behavior of $\langle p_T\rangle$. However, the main difference between our predictions and those presented in Ref. [9] comes from the model used to describe the QCD dynamics at high energies. This distinct behavior is present for pp and pPb collisions, with the behavior of the ratio at very large rapidities being determined by kinematical constraints associated with the limited phase space. These results were obtained considering $p_{T,\min} = 1$ GeV. In Fig. 5 we analyze the dependence of our results on this arbitrary

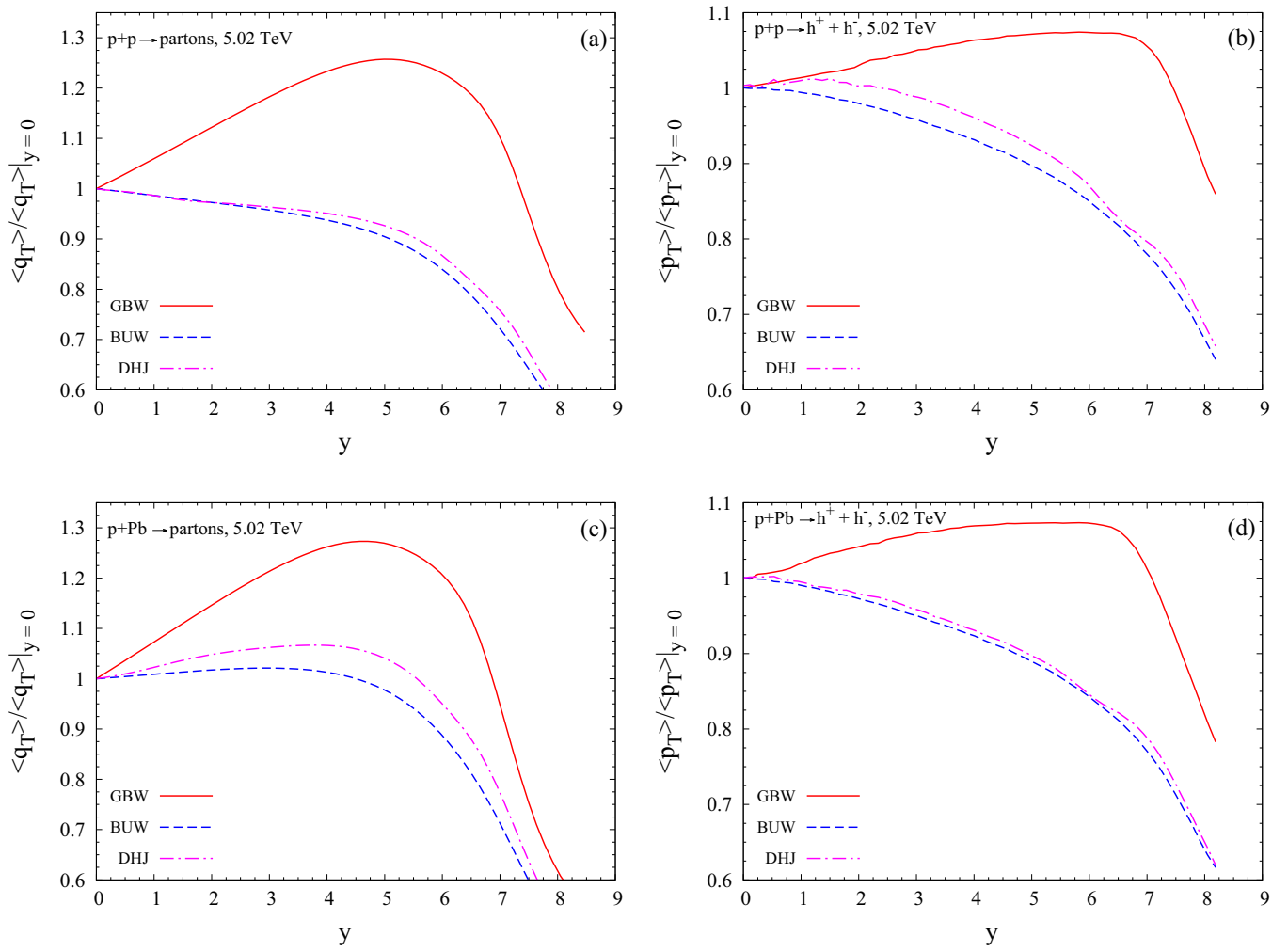

FIG. 4. Dependence of the ratio $\langle p_T(y,\sqrt{s})\rangle/\langle p_T(0,\sqrt{s})\rangle$ in the model used for the forward scattering amplitude in pp and pPb collisions. In panels (a) and (c) parton fragmentation is disregarded, while in (b) and (d) fragmentation is included.

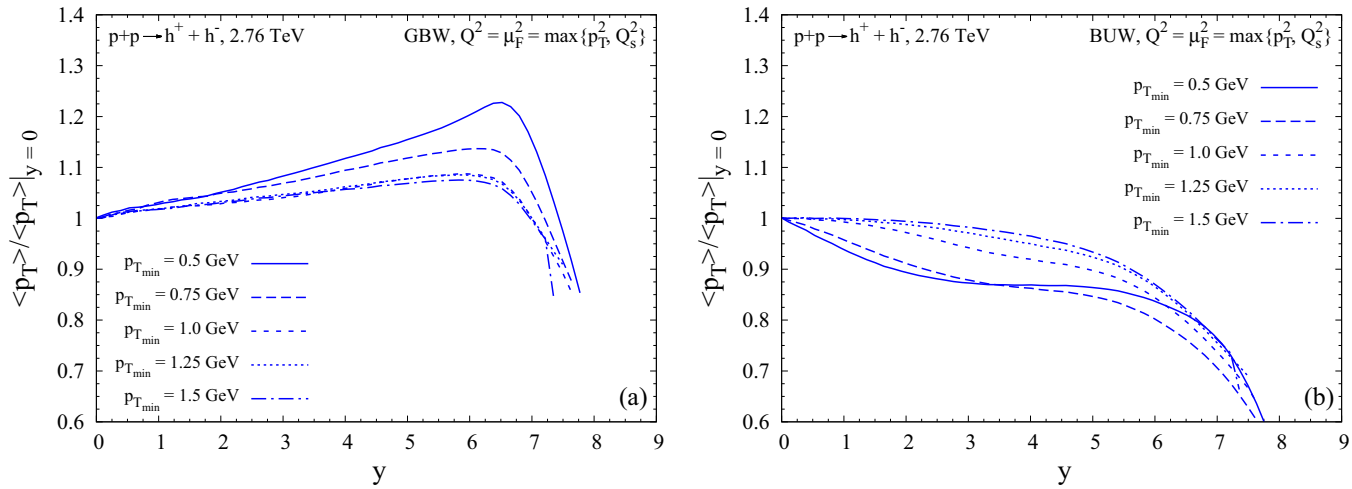

FIG. 5. Dependence of the ratio $\langle p_T(y,\sqrt{s})\rangle/\langle p_T(0,\sqrt{s})\rangle$ in the minimum transverse momentum $p_{T,\min}$ considering (a) the GBW and (b) the BUW model for the forward scattering amplitude.

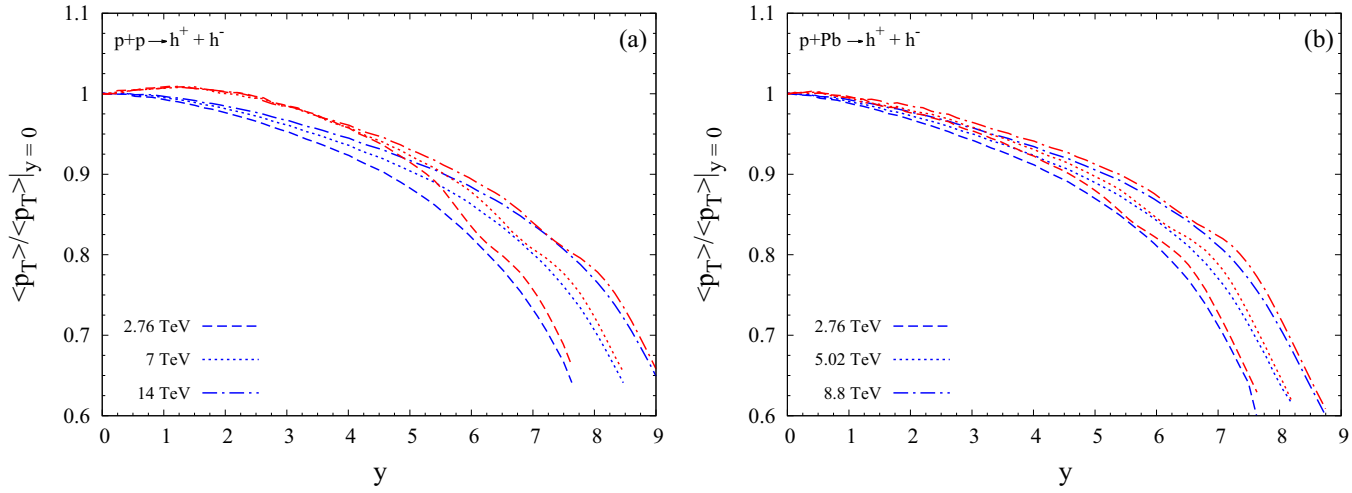

FIG. 6. Rapidity dependence of the ratio $R = \langle p_T(y,\sqrt{s})\rangle/\langle p_T(0,\sqrt{s})\rangle$ in (a) pp and (b) pPb collisions for different energies. The BUW (DHJ) predictions are represented by blue (red) lines.

cutoff in the transverse momentum. For this calculation we have compared the value of the saturation scale for a given transverse momentum and rapidity with the corresponding value of p_T and assumed that the factorization scale is given by the harder scale. This basic assumption has been used in Ref. [72] in order to extend the hybrid formalism to hadron production at very small p_T, obtaining a very good description of the LHCf data. However, it is important to emphasize that we have checked that similar results are obtained if we freeze the factorization scale at the minimum value of Q^2 allowed in the parton distributions and fragmentation functions when smaller values of p_T are probed in the calculation. The results shown in Fig. 5 indicate that the behavior of the ratio with rapidity is not strongly modified by the choice of $p_{T,\mathrm{min}}$. Consequently, we will consider $p_{T,\mathrm{min}} = 1$ GeV in what follows.

In Fig. 6 we present the behavior ratio $\langle p_T(y,\sqrt{s})\rangle/\langle p_T(0,\sqrt{s})\rangle$ for pp and pPb collisions considering different center-of-mass energies. We find that the predictions of the DHJ (red lines) and BUW (blue lines) are similar, with the DHJ being slightly larger than the BUW, and that the ratio increases with energy. Moreover, we observe that for a fixed energy the ratio is larger for pp in comparison to pPb collisions, as demonstrated in Fig. 7 where we present our results for the ratio between the predictions for $R = \langle p_T(y,\sqrt{s})\rangle/\langle p_T(0,\sqrt{s})\rangle$ in pp collisions and those obtained for pPb collisions. Our results indicate that at very large energies the predictions for R in pp and pPb collisions become identical. These predictions are an important test of the hybrid factorization and the CGC formalism. We believe that the analysis of the ratio R in pp and pPb collisions can be useful to probe the QCD dynamics at forward rapidities. Finally, the results from Fig. 6 indicate that the ratio decreases with the rapidity in pPb collisions for the energies probed by LHC, presenting a behavior similar to that obtained using a hydrodynamical approach, which implies that in principle this observable cannot be used to discriminate the CGC and hydrodynamical approaches for the description of the high=multiplicity events.

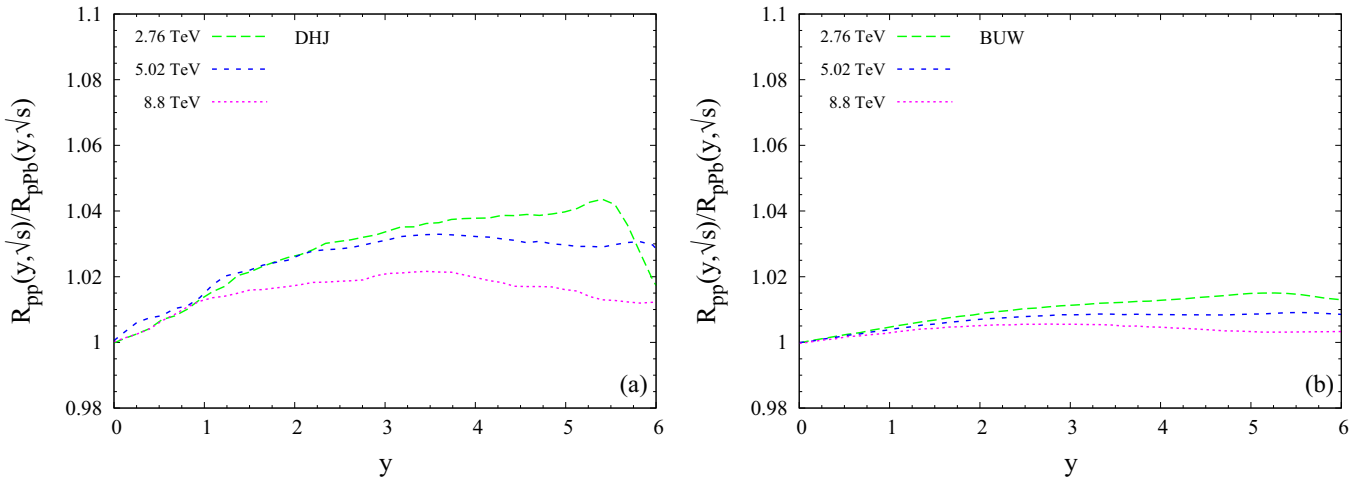

FIG. 7. Rapidity dependence of the ratio between the predictions for the $R = \langle p_T(y,\sqrt{s})\rangle/\langle p_T(0,\sqrt{s})\rangle$ in pp collisions and those for pPb collisions considering (a) the DHJ and (b) the BUW models.

This conclusion is opposite to that obtained in Ref. [9]. This difference comes from several facts. First, the CGC results in Ref. [9] were obtained using an analytical approximation for a particular unintegrated gluon distribution that does not describe (even at a qualitative level) the experimentally measured p_T spectra. Second, the calculation presented in [9] does not include the important contribution of the fragmentation processes to the average transverse momentum. Finally, kinematical constraints associated with phase-space restrictions at large rapidities were not included in [9] and, even in a partonic scenario, they play an important role at very large rapidities. In contrast, in our analysis we have calculated the ratio R using two different models for the forward scattering amplitude that are able to describe the current experimental data on charged hadron and pion p_T spectra measured in pp and pPb collisions at LHC. We have included the effects of parton fragmentation and phase-space restrictions. It is important to emphasize that although we have used the hybrid formalism instead of the k_T-factorization approach, we have verified that both approaches imply a similar behavior for the ratio R when the GBW model is used as input and the parton fragmentation is not taken into account. Our results demonstrate that the main difference comes from the treatment of the QCD dynamics at high energies.

IV. CONCLUSIONS

In this paper we considered the hybrid formalism to study the behavior of the average p_T with the rapidity in pp and pPb collisions at several energies in the CGC picture of high-energy collisions. To obtain realistic predictions we updated previous phenomenological models for the forward scattering amplitude, one with and one without geometric scaling violations. After constraining their parameters with the most recent data on the p_T spectra of charged particles, measured in pPb collisions at the LHC, we demonstrated that they are able to describe the recent pp data on the charged hadron and pion p_T spectra measured at LHC in the kinematical range of $p_T \leqslant 20$ GeV. Comparison of their predictions with the HERA and RHIC data were also presented. Using these models as input, we calculated the average transverse momentum $\langle p_T(y,\sqrt{s})\rangle$ in pp and pPb collisions, and estimated the energy and rapidity dependencies of the $R = \frac{\langle p_T(y,\sqrt{s})\rangle}{\langle p_T(0,\sqrt{s})\rangle}$, which is an observable that can be analyzed experimentally. We demonstrated that this ratio increases with energy for a fixed rapidity and decreases with rapidity for a fixed energy, with a behavior similar to that predicted in hydrodynamical approaches for high-multiplicity events. Our results indicated that this decreasing comes from the treatment of the QCD dynamics at high energies and the inclusion of the fragmentation process and kinematical constraints associated with the phase-space restrictions at very large rapidities. Finally, we demonstrated that these behaviors are very similar in pp and pPb collisions.

ACKNOWLEDGMENTS

We thank Daniël Boer for very instructive discussions. This work was partially financed by the Brazilian funding agencies CAPES, CNPq, FAPESP, and FAPERGS.

[1] F. Gelis, E. Iancu, J. Jalilian-Marian, and R. Venugopalan, Annu. Rev. Nucl. Part. Sci. **60**, 463 (2010); E. Iancu and R. Venugopalan, arXiv:hep-ph/0303204; H. Weigert, Prog. Part. Nucl. Phys. **55**, 461 (2005); J. Jalilian-Marian and Y. V. Kovchegov, *ibid.* **56**, 104 (2006).

[2] K. Akiba *et al.* (The LHC Forward Physics Working Group), LHC Forward Physics, CERN-PH-LPCC-2015-001 (unpublished).

[3] I. I. Balitsky, Nucl. Phys. B **463**, 99 (1996); Phys. Rev. Lett. **81**, 2024 (1998); Phys. Rev. D **60**, 014020 (1999); Phys. Lett. B **518**, 235 (2001).

[4] Y. V. Kovchegov, Phys. Rev. D **60**, 034008 (1999); **61**, 074018 (2000).

[5] J. Jalilian-Marian, A. Kovner, L. McLerran, and H. Weigert, Phys. Rev. D **55**, 5414 (1997); J. Jalilian-Marian, A. Kovner, A. Leonidov, and H. Weigert, *ibid.* **59**, 014014 (1998); J. Jalilian-Marian, A. Kovner, and H. Weigert, *ibid.* **59**, 014015 (1998); **59**, 034007 (1999); E. Iancu, A. Leonidov, and L. McLerran, Nucl. Phys. A **692**, 583 (2001); E. Ferreiro, E. Iancu, A. Leonidov, and L. McLerran, *ibid.* **701**, 489 (2002); H. Weigert, *ibid.* **703**, 823 (2002).

[6] J. Jalilian-Marian, Nucl. Phys. A **812**, 140 (2008).

[7] L. McLerran, M. Praszalowicz, and B. Schenke, Nucl. Phys. A **916**, 210 (2013).

[8] A. H. Rezaeian, Phys. Lett. B **727**, 218 (2013).

[9] P. Bozek, A. Bzdak, and V. Skokov, Phys. Lett. B **728**, 662 (2014).

[10] V. Khachatryan *et al.* (CMS Collaboration), J. High Energy Phys. 09 (2010) 091.

[11] S. Chatrchyan *et al.* (CMS Collaboration), Phys. Lett. B **718**, 795 (2013).

[12] B. Abelev *et al.* (ALICE Collaboration), Phys. Lett. B **719**, 29 (2013).

[13] G. Aad *et al.* (ATLAS Collaboration), Phys. Rev. Lett. **110**, 182302 (2013).

[14] B. B. Abelev *et al.* (ALICE Collaboration), Phys. Lett. B **726**, 164 (2013).

[15] A. Adare *et al.* (PHENIX Collaboration), Phys. Rev. Lett. **111**, 212301 (2013).

[16] L. Adamczyk *et al.* (STAR Collaboration), Phys. Lett. B **743**, 333 (2015).

[17] S. Chatrchyan *et al.* (CMS Collaboration), Phys. Lett. B **724**, 213 (2013).

[18] B. Alver and G. Roland, Phys. Rev. C **81**, 054905 (2010); **82**, 039903 (2010).

[19] L. Adamczyk *et al.* (STAR Collaboration), Phys. Rev. C **88**, 014904 (2013).

[20] P. Bozek, Eur. Phys. J. C **71**, 1530 (2011); P. Bozek and W. Broniowski, Phys. Lett. B **718**, 1557 (2013); Phys. Rev. C **88**, 014903 (2013).

[21] P. Bozek, W. Broniowski, and G. Torrieri, Phys. Rev. Lett. **111**, 172303 (2013).

[22] A. Dumitru, F. Gelis, L. McLerran, and R. Venugopalan, Nucl. Phys. A **810**, 91 (2008); S. Gavin, L.

McLerran, and G. Moschelli, Phys. Rev. C **79**, 051902 (2009).
[23] A. Dumitru, K. Dusling, F. Gelis, J. Jalilian-Marian, T. Lappi, and Venugopalan, Phys. Lett. B **697**, 21 (2011).
[24] A. Dumitru and J. Jalilian-Marian, Phys. Rev. D **81**, 094015 (2010).
[25] A. Kovner and M. Lublinsky, Phys. Rev. D **83**, 034017 (2011); **84**, 094011 (2011).
[26] E. Levin and A. H. Rezaeian, Phys. Rev. D **84**, 034031 (2011).
[27] E. Iancu and D. Triantafyllopoulos, J. High Energy Phys. 11 (2011) 105.
[28] K. Dusling and R. Venugopalan, Phys. Rev. D **87**, 094034 (2013); **87**, 054014 (2013).
[29] Y. V. Kovchegov and D. E. Wertepny, Nucl. Phys. A **925**, 254 (2014).
[30] R. L. Ray, Phys. Rev. D **84**, 034020 (2011); **90**, 054013 (2014).
[31] A. Dumitru, L. McLerran, and V. Skokov, Phys. Lett. B **743**, 134 (2015).
[32] A. Kovner and A. H. Rezaeian, Phys. Rev. D **92**, 074045 (2015).
[33] G. Aad *et al.* (ATLAS Collaboration), Phys. Lett. B **725**, 60 (2013); The ATLAS Collaboration, ATLAS-CONF-2014-021 (unpublished).
[34] P. Bozek, Phys. Rev. C **85**, 014911 (2012); A. Bzdak, B. Schenke, P. Tribedy, and R. Venugopalan, *ibid.* **87**, 064906 (2013); E. Shuryak and I. Zahed, *ibid.* **88**, 044915 (2013); K. Werner, M. Bleicher, B. Guiot, I. Karpenko, and T. Pierog, Phys. Rev. Lett. **112**, 232301 (2014); B. Schenke and R. Venugopalan, *ibid.* **113**, 102301 (2014).
[35] A. Dumitru and A. V. Giannini, Nucl. Phys. A **933**, 212 (2014); T. Lappi, Phys. Lett. B **744**, 315 (2015); B. Schenke, S. Schlichting, and R. Venugopalan, *ibid.* **747**, 76 (2015); A. Dumitru, A. V. Giannini, and V. Skokov, arXiv:1503.03897; T. Lappi, B. Schenke, S. Schlichting, and R. Venugopalan, J. High Energy Phys. 061 (2016) 1601.
[36] K. J. Golec-Biernat and M. Wusthoff, Phys. Rev. D **59**, 014017 (1998).
[37] Yu. Dokshitzer, Sov. Phys. JETP **46**, 641 (1977); V. N. Gribov and L. N. Lipatov, Sov. J. Nucl. Phys. **15**, 438 (1972); G. Altarelli and G. Parisi, Nucl. Phys. B **126**, 298 (1977).
[38] L. N. Lipatov, Sov. J. Nucl. Phys. **23**, 338 (1976); E. A. Kuraev, L. N. Lipatov, and V. S. Fadin, Sov. Phys. JETP **45**, 199 (1977); I. I. Balitsky and L. N. Lipatov, Sov. J. Nucl. Phys. **28**, 822 (1978).
[39] E. Iancu, C. Marquet, and G. Soyez, Nucl. Phys. A **780**, 52 (2006).
[40] A. Dumitru, A. Hayashigaki, and J. Jalilian-Marian, Nucl. Phys. A **765**, 464 (2006); **770**, 57 (2006).
[41] D. Boer, A. Utermann, and E. Wessels, Phys. Rev. D **77**, 054014 (2008).
[42] T. Altinoluk and A. Kovner, Phys. Rev. D **83**, 105004 (2011).
[43] G. A. Chirilli, B.-W. Xiao, and F. Yuan, Phys. Rev. Lett. **108**, 122301 (2012).
[44] G. A. Chirilli, B. W. Xiao, and F. Yuan, Phys. Rev. D **86**, 054005 (2012).
[45] J. L. Albacete, A. Dumitru, H. Fujii, and Y. Nara, Nucl. Phys. A **897**, 1 (2013).
[46] J. L. Albacete, N. Armesto, J. G. Milhano, and C. A. Salgado, Phys. Rev. D **80**, 034031 (2009).
[47] J. Kuokkanen, K. Rummukainen, and H. Weigert, Nucl. Phys. A **875**, 29 (2012).
[48] T. Lappi and H. Mantysaari, Phys. Rev. D **91**, 074016 (2015).
[49] J. L. Albacete and C. Marquet, Phys. Lett. B **687**, 174 (2010).
[50] J. Jalilian-Marian and A. H. Rezaeian, Phys. Rev. D **85**, 014017 (2012); A. H. Rezaeian, Phys. Lett. B **718**, 1058 (2013)
[51] T. Lappi and H. Mantysaari, Phys. Rev. D **88**, 114020 (2013)
[52] P. Tribedy and R. Venugopalan, Phys. Lett. B **710**, 125 (2012); **718**, 1154 (2013).
[53] D. Kharzeev, Y. V. Kovchegov, and K. Tuchin, Phys. Lett. B **599**, 23 (2004).
[54] J. Bartels, K. Golec-Biernat, and H. Kowalski, Phys. Rev. D **66**, 014001 (2002); H. Kowalski and D. Teaney, *ibid.* **68**, 114005 (2003); E. Iancu, K. Itakura, and S. Munier, Phys. Lett. B **590**, 199 (2004); H. Kowalski, L. Motyka, and G. Watt, Phys. Rev. D **74**, 074016 (2006); V. P. Goncalves, M. S. Kugeratski, M. V. T. Machado, and F. S. Navarra, Phys. Lett. B **643**, 273 (2006); C. Marquet, R. Peschanski, and G. Soyez, Phys. Rev. D **76**, 034011 (2007); G. Soyez, Phys. Lett. B **655**, 32 (2007); G. Watt and H. Kowalski, Phys. Rev. D **78**, 014016 (2008).
[55] M. A. Betemps and V. P. Goncalves, J. High Energy Phys. 09 (2008) 019.
[56] A. M. Stasto, K. Golec-Biernat, and J. Kwieciński, Phys. Rev. Lett. **86**, 596 (2001).
[57] C. Marquet and L. Schoeffel, Phys. Lett. B **639**, 471 (2006).
[58] V. P. Goncalves and M. V. T. Machado, Phys. Rev. Lett. **91**, 202002 (2003); J. High Energy Phys. 04 (2007) 028.
[59] B. Abelev *et al.* (ALICE Collaboration), Phys. Rev. Lett. **110**, 082302 (2013).
[60] A. H. Rezaeian and I. Schmidt, Phys. Rev. D **88**, 074016 (2013).
[61] F. O. Durães, A. V. Giannini, V. P. Gonçalves, and F. S. Navarra, Phys. Rev. C **89**, 035205 (2014).
[62] J. Pumplin, D. R. Stump, J. Huston, H. L. Lai, P. M. Nadolsky, and W. K. Tung, J. High Energy Phys. 07 (2002) 012.
[63] B. A. Kniehl, G. Kramer, and B. Pötter, Nucl. Phys. B **582**, 514 (2000).
[64] G. P. Salam, J. High Energy Phys. 07 (1998) 019; M. Ciafaloni, D. Colferai, and G. P. Salam, Phys. Rev. D **60**, 114036 (1999).
[65] B. B. Abelev *et al.* (ALICE Collaboration), Eur. Phys. J. C **73**, 2662 (2013).
[66] G. Aad *et al.* (ATLAS Collaboration), Phys. Lett. B **688**, 21 (2010); New J. Phys. **13**, 053033 (2011).
[67] V. Khachatryan *et al.* (CMS Collaboration), J. High Energy Phys. 02 (2010) 041; S. Chatrchyan *et al.* (CMS Collaboration), *ibid.* 08 (2011) 086; V. Khachatryan *et al.* (CMS Collaboration), Phys. Rev. Lett. **105**, 022002 (2010).
[68] B. I. Abelev *et al.* (ALICE Collaboration), Phys. Lett. B **717**, 162 (2012).
[69] B. I. Abelev *et al.* (STAR Collaboration), Phys. Rev. D **80**, 111108 (2009).
[70] J. Adams *et al.* (STAR Collaboration), Phys. Rev. Lett. **91**, 072304 (2003); I. Arsene *et al.* (BRAHMS Collaboration), *ibid.* **93**, 242303 (2004); J. Adams *et al.* (STAR Collaboration), *ibid.* **97**, 152302 (2006).
[71] S. Aid *et al.* (H1 Collaboration), Nucl. Phys. B **470**, 3 (1996); M. Derrick *et al.* (ZEUS Collaboration), Z. Phys. C **72**, 399 (1996); C. Adloff *et al.* (H1 Collaboration), Nucl. Phys. B **497**, 3 (1997); J. Breitweg *et al.* (ZEUS Collaboration), Phys. Lett. B **407**, 432 (1997); **487**, 53 (2000); C. Adloff *et al.* (H1 Collaboration), Eur. Phys. J. C **21**, 33 (2001); S. Chekanov *et al.* (ZEUS Collaboration), *ibid.* **21**, 443 (2001).
[72] V. P. Goncalves and M. L. L. da Silva, Nucl. Phys. A **906**, 28 (2013).